Supplemental Information

Supplemental Methods

Mice

We measured gap detection behavior in heterozygous offspring (both males and females) of crosses between a cre-dependent Arch line, CAG-Arch-eGFP (JAX No. 012735), and two interneuron lines: Pvalb-IRES-Cre ("PV", n=5, JAX No. 008069), or SOM-IRES-Cre ("SOM", n=9, JAX No. 013044). We also measured gap detection behavior in mice expressing Arch in pyramidal neurons. These were generated by crossing a CaMKII-tTA line ("CaMKII", n=6, JAX No. 003010) to a tTA-dependent Arch line, which we report here for the first time. The generation of the line is described in Supplemental Materials ("*tetO-ArchT2 Generation*"). Matched Arch-negative littermates were used as behavioral controls (PV, n=2; SOM, n=3, CaMKII, n=2). Data were collected from a total of 70 mice, including those used in electrophysiological control experiments: coordinates for fiber optic placement were determined in 10 C57Bl/6 mice; electrophysiological verification of Arch was performed in 5 PV, 4 SOM, and 2 CaMKII mice; GTR manipulation was assessed in 3 SOM, 2 PV and 3 CaMKII mice; light intensity mapping was performed in 3 CaMKII mice; and measures of pre-pulse inhibition in 6 PV and 4 SOM mice. Expression density was measured in 2 PV, 2 SOM, and 5 CaMKII mice.

tetO-ArchT2 Generation

The ArchT2/GFP fusion gene was amplified from the Fck-gene 16 GFP construct courtesy of Ed Boyden using primers F 5'gctacttgtgattgctccat and R 5'gttctccatttgcactcagg. The ArchT2/GFP PCR product was ligated directionally into the tetO (Clontech) cassette using BamHI and SalI restriction enzymes. The resulting construct was digested with DrdI and XmnI and gel extracted using the QIAGEN gel extraction kit. The resulting 3283kb linear fragment contained the tetO promoter, ArchT2/GFP fusion gene, the WPRE element and the SV40 polyA. The fragment was suspended in filtered low TE and injected into DBA oocytes. A genotyping primer pair, F 5'ctgctgctaaggagaggggac and R 5'ggtgttctgctggtagtggtc, flank the junction between ArchT2 and GFP. The construct for the CaMKII line is shown in Figure S1.

Surgical Procedures

In the present study, separate surgical procedures were performed for determining optimal fiber coordinates ("Acute Surgery"), extent of suppression at different depths ("Acute Surgery"), electrophysiological verification ("Acute Surgery"), assessing the impact of suppression on the gap termination response ("GTR manipulation") and assessing gap detection with optogenetic suppression ("Fiber Implantation"). All surgeries were performed using aseptic techniques.

Acute Surgery

Mice were anesthetized with 120–180mg/kg ketamine, 0.24–0.36mg/kg medetomidine, and 0–4.5mg/kg acepromazine, by i.p. injection; the dose was adjusted to eliminate the pedal withdrawal reflex. Anesthetics were supplemented as necessary to maintain depth of anesthesia. Dexamethasone (0.1mg/Kg) and atropine (0.03mg/Kg) were administered to reduce inflammation and respiratory irregularities, respectively. Dilute 0.1%–0.5% lidocaine, not exceeding 5mg/kg, was topically applied where pressure would be applied, or incisions made. Body temperature was maintained at 37°C. The head was held in a custom apparatus that clamped both orbits and the palate, leaving the ears unobstructed. A cisternal drain was performed. The left auditory cortex was exposed, followed by a craniotomy and a durotomy. The cortical surface was covered with 4% agarose in saline (0.9% NaCl), and kept moist with saline.

GTR manipulation

Multi-unit recordings were performed in awake, head-fixed mice. Mice were surgically prepared as described above. The beveled end (45°) of an aluminum post (L: ~35mm; dia: 5mm) was cemented to the surface of the skull. A portion of the skull overlying auditory cortex, left free of cement, was covered with Sylgard (Dow Corning, Midland, MI). All mice were individually housed following surgery and were allowed 7 days of post-operative recovery. Prior to recording, the Silgard was removed and the skull cleaned with saline. Lidocaine HCL gel (2%) was then applied to the surface of the skull. After five minutes, the gel was removed with saline, and the mouse transferred to the recording chamber.

Fiber Implantation

Dexamethasone (0.1mg/kg) and atropine (0.03mg/kg) were administered pre-surgically to reduce inflammation and respiratory irregularities, respectively. Surgical anesthesia was maintained with isoflurane (1.25-2.0%, adjusted as necessary). Body temperature was maintained at 37°C, and the eyes kept moist with a thin layer of ophthalmic ointment. Mice were positioned in a stereotaxic frame. The skull was then exposed, and lambda and bregma zeroed in the vertical plane. A thin film of cyanoacrylate was spread over the surface of the skull. One hole was drilled in each hemisphere at the coordinates derived from cortical mapping (AP: -2.2mm, ML: 4.4mm, relative to bregma; Fig. S2) and optic fibers (200µm-diameter) were positioned over auditory cortex (depth 0.5mm below the dura, see Fig. S3). Grip cement was used to secure the fibers to the skull, bonding with the cyanoacrylate. Ketoprofen (4.0mg/kg) was administered post-operatively to minimize discomfort. Mice were housed individually following the surgery and were allowed 7 days of post-operative recovery.

Data Acquisition and Analysis

Fiber Coordinate Mapping

To determine the coordinates for fiber optic placements in implanted mice, we marked the limits of robustly white noise responsive areas with a Methylene Blue coated electrode and obtained their stereotaxic coordinates, postmortem. The boundary points were marked following our standard mapping procedure: for each animal we obtained a coarse map of auditory cortex, using both multi-unit responses and evoked local field potentials from the middle cortical layers (150-450μm). We assessed the tuning and white noise responses of recording sites using a frequency-intensity tuning curve (tones from 1-40kHz at 4 frequencies/octave, plus white noise, presented at 20-80dB in 15dB steps, and with ≥15 repetitions). Auditory core fields (AI and AAF) were identified by a caudal-to-rostral reversal in tonotopy, bounded by white noise responsive sites with poor or disordered frequency tuning [S1].

Light Intensity Mapping

To determine the optimal light power for suppressing activity in auditory cortex, we measured suppression in CaMKII mice at a range of depths and laser intensities. To match the light conditions in the behavioral experiments, mice were first implanted with 200μm fibers in a stereotaxic frame (see "*Fiber Implantation*"). The animals were then transferred to the recording head-holder and the acute surgery was performed. For these experiments we positioned a tungsten microelectrode (2-5MΩ) immediately beside, and approximately parallel to, the optic fiber. We systematically tested the efficacy of the laser in suppressing spontaneous spiking activity at different intensities and depths (100-1000mW/mm^2; 500-2500μm). The stimulus consisted of a 300ms window, during which the laser was either "on" or "off", on interleaved trials (≥40 repetitions, 500ms ISI). The effect of laser illumination was calculated as a paired *t*-test comparing spike counts during "on" and "off" windows. Multiple penetrations were made in each animal. "Percent suppression" (Fig. S3) is the fraction of recordings at each depth where spontaneous activity was significantly suppressed.

GTR manipulation

Mice were placed on a 12cm X 15cm sheet of PTFE inclined at ~20° and the aluminum post fixed in position, immobilizing the head. This allowed for freedom of movement while maintaining physical stability for recordings. A low impedance (~2-4MΩ) sharp tungsten electrode was inserted through a small opening in the skull. Activity was monitored in the presence of white noise pulses. Upon detecting white noise responses, a session was initiated. High-pass filtered (300-10kHz) multi-unit data were collected during 72 presentations (36 laser "on" and 36 laser "off") of alternating 0ms and 10ms gaps

paired with 25ms startle pulse (separated by a 50ms post-gap interval). The minimum amplitude threshold for the analysis of multi-unit activity was >3 SD of the baseline extracellular voltage. Data were analyzed only from those recording sessions during which 1) significant GTRs were detected, as revealed by paired *t*-test with a corresponding 50ms pre-gap baseline window, and 2) no differences between laser "on" and "off" baselines were observed (unpaired *t*-test). Data were binned (5ms), and the effects of the laser were established using unpaired *t*-tests comparing the post-gap interval for laser "on" and "off" trials. Multiple recordings were taken at different depths during a single penetration. Diluted Nutri-Cal (Vetoquinol, Princeville, Quebec, Canada) was administered orally between recording sessions.

Behavioral Methods: Sound and Light Delivery and Control

The speaker was calibrated to within ±1 dB using a Brüel and Kjær 4939 ¼" microphone positioned where the ear would be, without the animal present. The tube was perforated (~3mm dia.) to allow effective transmission of sound, with no more than 5dB attenuation. An open slot along the top provided access to the implanted fibers. During gap detection sessions, two flexible fiber optic tethers (3m length, 200µm diameter, Doric Lenses, Quebec, Canada) delivered light from two custom-built lasers (max output 150mW, 532nm) to the fibers implanted in each animal. Illumination was gated by a TTL-driven shutter. To reduce the likelihood of the animal being visually cued by any stray laser illumination during gap detection, the grip cement was coated with a layer of black latex paint, and ambient green light strobed continuously throughout the entire session.

White noise served as both the continuous background (80dB SPL) and startle stimulus (25ms burst, 100dB SPL). Startle stimuli were separated by a random intertrial interval of 15 ± 5s. Gaps in the continuous background noise preceded the startle stimulus. The interval between the end of the gap and the onset of the startle stimulus was 50ms. We assessed detection of gaps 0-10ms in duration, in 2ms increments (where 0ms indicates a trial without a gap). In a given session, each gap duration was presented 24 times: 12 with and 12 without optogenetic suppression, in interleaved trials. In each session, gap-associated changes in startle amplitude were compared to the response to the startle stimulus without a preceding gap ("0ms gap"). The ability to detect longer gaps, 25ms or 50ms in duration, was assessed in separate behavioral sessions due to time constraints (72 presentations of each, 36 with and 36 without suppression).

Histological Procedures

Antibody Labeling

We quantified Arch expression in the interneuron crosses by co-localization of its native fluorescence with antibody labeling for parvalbumin or somatostatin. 30µm thaw-mounted sections were first blocked in 10% normal goat or donkey serum with 0.3% triton in PBS for three hours at room temperature. Sections were incubated overnight at 4°C with a primary antibody for PV (mouse anti-parvalbumin, 1:4000, Millipore MAB1572) or SOM (rat anti-somatostatin, 1:200, Millipore MAB354), followed by four hours of room temperature incubation with a fluorescent-labeled secondary antibody (PV: Alexa Fluor 546 goat anti-mouse, 1:400, Invitrogen A11003; SOM: Alexa Fluor 546 donkey anti-rat, 1:100, A11081).

in situ *Hybridization*

We quantified Arch expression in the CaMKII cross by co-localization of the ArchT2 and CaMKII sequences, visualized using nonradioactive dual *in situ* hybridization (Tyramide Signal Amplification, NEN Life Science Products). For CaMKII, we used a digoxygenin (DIG)-labeled riboprobe (1:500), visualized by Anti Fluor-POD (1:1000; Invitrogen, Cat. A21253) and Fluorescein (1:50; PerkinElmer, Cat. NEL741). For ArchT2, we used a FITC-pWPRE riboprobe (1:1000), visualized by Anti-Digoxigenin-POD (1:1000; Roche, Cat. 1207733910) and Cyanine 3 (1:50; PerkinElmer, Cat. NEL744). 30µm thaw-mounted sections were hybridized overnight at 62ºC with the DIG and FITC-pWPRE riboprobes, and then incubated at room temperature for 4 hours in blocking solution (TBST buffer + 0.5% blocking reagent, PerkinElmer TSA kit). The anti-Fluor-POD antibody was added and the sections were incubated overnight at room temperature. The tissue was washed with TBST buffer, exposed to Fluorescein for 45' at room temperature, and incubated for 4 hours in blocking solution. The sections then incubated overnight in anti-digoxegenin-POD antibody at 4°C. The tissue was exposed to Cyanine 3 for 45' at room temperature, then washed in TBST buffer.

Quantification of Expression Specificity

Expression specificity was quantified within a 250µm wide strip of primary auditory cortex extending from the pia to the white matter. Cells were identified in independent fluorescence channels and subsequently scored for co-localization. Cells were identified at 20X magnification on the basis of morphology and the presence of processes extending from the soma. To estimate the cell density as a function of cortical depth, cell counts were taken in 50µm bins throughout the cortical depth as reported in Figs. 1B, 2B, 3B. Thus, cell density is reported as cells/bin where the bin corresponds to a 250µm x 50µm bin. The 250µm strips were systematically positioned over auditory cortex based on the shape of the hippocampus in the coronal sections. Coordinates of the strips were: SOM: AP = -2.3 ± 0.17SD, and

1.54 ± 0.11SD above the rhinal fissure. PV: AP = -2.4 ± 0.18SD, and 1.35 ± .2SD above the rhinal fissure. CaMKII: AP = -2.3 ± .16SD, and 1.3 ± .22SD above the rhinal fissure.

Data Acquisition and Stimuli

Electrophysiological data were collected in a sound-attenuating chamber. We recorded from left auditory cortex and presented sounds to the contralateral ear. The speaker was calibrated before each experiment. The acoustic stimuli were pure tones or white noise bursts 25ms in duration with 3ms ramps. Stimuli were pseudorandomly interleaved and separated by an interstimulus interval (ISI) ≥500ms. Multi-unit recordings were obtained using 2-5MΩ tungsten microelectrodes and amplified with an A-M Systems 1800 amplifier (band-pass filtered 300–5000Hz). Single-unit recordings were obtained using the loose cell-attached patch method, using 3-4MΩ glass pipettes filled with a 0.9% saline internal solution, and amplified with Axopatch 200b amplifier. Spikes were extracted offline using a fixed voltage threshold at least 3 SD above the baseline extracellular voltage. Subpial recording depths were determined from micromanipulator travel.

Electrophysiological Verification

We confirmed that Arch activation had the anticipated effect on neural activity in auditory cortex – that is, an increase in activity due to the suppression of inhibitory neurons (PV, SOM), or a decrease in activity due to the suppression of pyramidal excitatory cells (CaMKII). In these experiments the optical fiber was positioned directly over the craniotomy. We surveyed the effect of illumination (300mW/mm^2) on single-unit and multi-unit responses throughout the depth of auditory cortex (100-950μm; core auditory cortex identified as described above). The stimulus consisted of a 25ms white noise burst, embedded on interleaved trials in a 150ms or 300ms laser pulse (≥20 repetitions). The effect of illumination on driven activity was calculated with a paired *t*-test comparing spike counts between laser "on" and "off" trials, in the 100ms window following sound onset. The effect of illumination on spontaneous activity was calculated similarly, but in the 50 or 100 ms window preceding sound onset.

Circuit Model

We implemented a simple circuit model that qualitatively captured the structure of our results. The model (Fig. 4A, inset) consisted of a sound envelope *s*, with 0-10ms silent gaps embedded in Gaussian white noise, which served as input to a pyramidal (excitatory) neuron (PN) and an inhibitory interneuron (IN). The inhibitory neuron integrated its input with an exponentially weighted window,

$$IN_t = \frac{1}{N}\sum_{a=0}^{\infty} s_{t-a} e^{-\frac{a}{\tau}}$$

where N is a normalizing constant, $N = \sum_{0}^{\infty} e^{-\frac{t}{\tau}}$, and the time constant τ was 25ms. Varying τ from 5-100ms changed the steepness of the gap detection curves (e.g., Fig. 4B) but did not otherwise affect the results. The PN integrated the sound input and subtractive inhibition, $PN = s - IN$ [S2]. The PN output was band-pass filtered (10-300Hz) and thresholded at 0 to produce non-negative output. Varying filter cutoffs or thresholds over a wide range did not affect the results. The PN output then served as input to a second PN and IN pair, identical to the first. The output of the second PN was converted to behavioral performance according to

$$\%\ startle = 100\left(1 - \frac{\max(PN)}{k}\right)$$

where k is an arbitrary constant that sets the asymptotic gap performance for long gaps. We used $k = 10$ to approximate the performance levels of our mice, although varying k from 1-100 did not qualitatively affect the results. We modeled optogenetic suppression as a subtractive term applied to either the first PN (Fig. 4A, inset), or the second IN (Fig. 5A, inset). Varying the magnitude of the optogenetic term by several-fold changed the strength of the effect, but did not qualitatively affect the results. We also tried a much simpler model architecture, with only sound, a single PN and an IN [2], which also reproduced the effects of pre-gap, post-gap, and prolonged suppression. Here we used the two-layer model because it allowed us to conceptually separate the cortical neurons being optogenetically suppressed from the sound input and behavioral output layers.

Supplemental Results

Fiber Coordinate Mapping

We experimentally determined the optimal fiber coordinates for delivering light throughout mouse auditory cortex. We used multi-unit recordings to map white noise responsiveness in 10 mice, aged 13 ± 2 weeks SE. White noise responsive regions extended, on average, from 1.5mm to 2.8mm caudal to bregma (Fig. S2), centered at 2.2 ± 0.09mm caudal to bregma and 4.9 ± 0.11mm lateral to the midline (mean ± SE), measured at the cortical surface. Based on these data, we chose to implant single optic fibers bilaterally 2.2mm caudal to bregma and 4.4mm lateral to the midline, at a depth of 0.5mm, so that the fibers were directly over the middle cortical layers (Fig. S3). All fiber placements were verified postmortem to be directly over auditory cortex.

To further test whether any variability in fiber placement affected our results, we compared effect sizes within and across animals. If fiber placement were contributing to our results, we would expect that the variance across animals would be greater than the variance within individual animals (across sessions). In

other words, some animals might show large effects, others small effects, averaging out to a modest effect size. In contrast, if our fiber placements were consistently accurate, we would expect that the variance across animals would be about the same as the variance within individual animals (across sessions). In other words, all animals would show consistently modest effect sizes. We found the latter. We measured the effect of post-gap laser on % startle response for a 10ms gap, and asked whether there was a significant difference between animals, using the ANOVA, with Bonferroni correction if there were 3 or more mice in the ANOVA. There were no significant ANOVAs for any of our mouse lines or laser powers. This suggests that variability in fiber placement is not strongly contributing to our results.

Light Intensity Mapping

We experimentally determined the optimal light power for suppressing activity in auditory cortex. This was accomplished by measuring suppression at a range of depths and laser intensities in 3 anesthetized CaMKII mice implanted with fibers as in our behavioral experiments (Fig. S2). Atlas coordinates [S3] and our cortical mapping results indicated that a volume 1.5mm in diameter from the tip of the fiber should target auditory cortex, but not adjacent structures. A roughly spherical region of suppression was expected based on previously modeled results [S4]. We tested six intensities (100-1000mW/mm^2, measured at the fiber tip; Fig. S3A). Figure S3B shows the suppression of spontaneous spiking, and the calculated irradiance, as a function of depth for laser intensities of 300 and 1000mW/mm^2 (irradiance calculation: http://www.openoptogenetics.org). We found that 300mW/mm^2 was the highest intensity for which suppression was limited to auditory cortex (i.e., spiking was unaffected >1.5 mm from the fiber tip). This intensity is comparable to those used in other *in vivo* studies [S4, 5, 6, 7]. The highest intensity (1000mW/mm^2 at the fiber tip) produced more robust suppression within auditory cortex, but also caused significant suppression of spontaneous activity at a depth of 2.5mm, outside of auditory cortex. We therefore used both intensities in subsequent experiments: 300mW/mm^2, which affected only auditory cortex and provided moderate suppression, and 1000mW/mm^2, which provided more robust suppression in auditory cortex but may have affected adjacent cortical and subcortical regions.

GTR Manipulation

In addition to verifying the electrophysiological efficacy of each line, we examined the impact of suppression (300mW/mm^2) directly on the GTR. The observed effects were consistent with our expectations. Suppression of SOM interneurons following a 10ms gap reliably increased GTR amplitudes (Fig. S4A). Significant increases in spiking activity were observed in 5 of 10 sites exhibiting a GTR (sites recorded from 3 mice, unpaired *t*-test). Suppression of PV interneurons similarly increased GTR amplitudes (Fig. S4B). Significant increases in spiking activity were observed in 5 of 8 sites exhibiting a

GTR (sites recorded from 2 mice). In contrast to the effects of interneuron suppression, and consistent with expectations, suppression of CaMKII-positive neurons significantly reduced the GTR following 10ms gaps at 5 of 10 sites at which GTRs were observed (Fig. S4C; sites recorded from 3 mice).

Consistency of Startle Reflexes and Gap Detection Across Trials and Sessions

The startle reflex was remarkably robust across trials, with no evidence of habituation. To demonstrate this, we compared startle responses (in the no-gap condition) across all trials within a session (Fig. S6). Startle response amplitude was very stable both across trials and between the first and last session for each animal. Experience-related modification of brief gap detection (2-5ms) has been reported previously in rats [S8], however a comparison (paired *t*-test) of gap-attenuated startle amplitudes following 2ms and 4ms gap durations on the first and last session for each mouse (in the absence of suppression) did not reveal an effect of experience. This justifies the inclusion of data from multiple sessions.

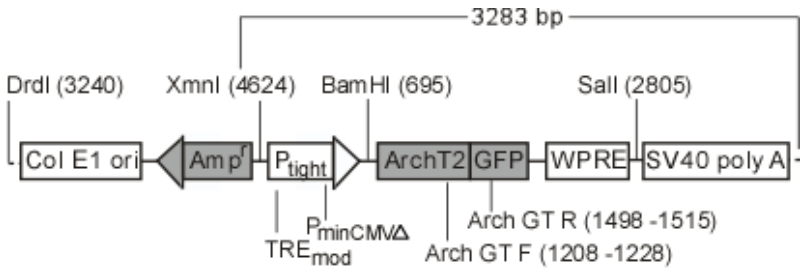

Figure S1. Injection construct for the ArchT2/GFP tetO line.

(Related to Experimental Procedures)

The construct containing the ArchT2/GFP fusion gene was injected into DBA oocytes and placed under control of a commercially available CaMKII promoter (B6;CBA-Tg(Camk2a-tTA)1Mmay/J, Jackson Labs 003010). Offspring expressed the Arch receptor throughout the forebrain.

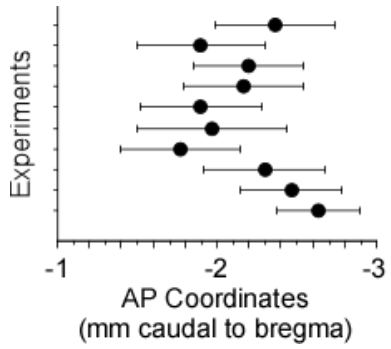

Figure S2. Mapping fiber coordinates for behavioral gap detection experiments.

(Related to Experimental Procedures)

We determined the approximate boundaries within auditory cortex showing robust white noise responses and coarse tonotopy. The center of these responsive regions ranged from 1.5 to 2.8mm caudal to bregma, with a mean at 2.2 ± .09mm. Data were collected from 10 anesthetized mice. Lines represent rostral-to-caudal distance determined for responsive regions in each animal.

Figure S3. Suppression at different depths and laser intensities.

(Related to Experimental Procedures)

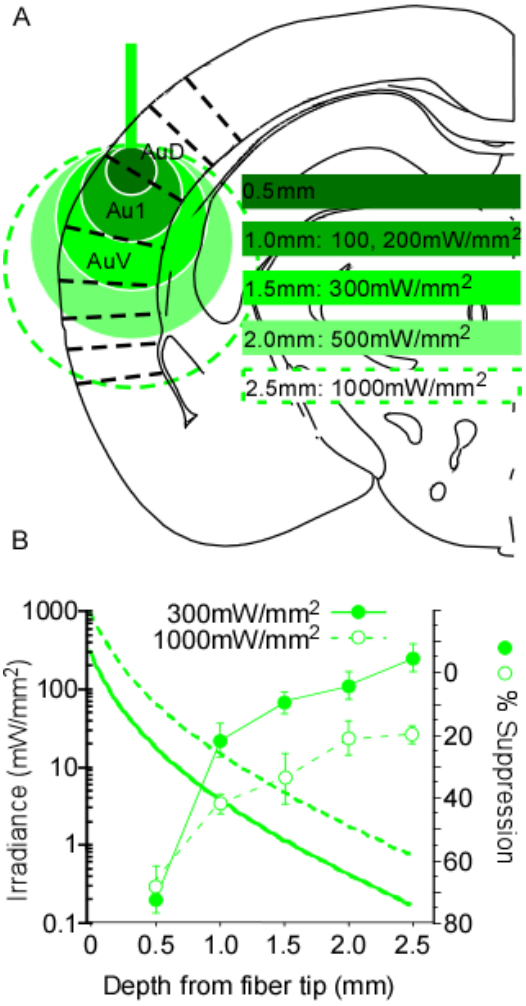

A) We measured suppression in anesthetized CaMKII mice, implanted with fibers as in our behavioral experiments, at fiber-tip intensities of 100, 200, 300, 500 and 1000mW/mm^2 and at recording depths of 500-2500µm, in 500µm increments. The minimum separation between fiber tip and recording electrode was 500 µm. We tested the efficacy of the laser in suppressing spontaneous multi-unit activity in a 300ms window (with interleaved "laser on" and "laser off" trials, unpaired *t*-test). The values listed indicate the greatest depth at which those intensities elicited significant suppression. We identified 300mW/mm^2 (at the fiber tip) as the optimal intensity for achieving balance between strength of suppression and restriction to auditory cortex. The dashed line indicates that a limit was not observed for the 1000mW/mm^2 intensity. Coronal section modified from Paxinos & Franklin, 2001. **B)** Percent suppression (right axis) decreased with recording depth, shown for the tip intensities used in the behavioral experiments (300mW/mm^2, solid; 1000mW/mm^2, dashed). Calculated irradiance is shown on the left axis. Suppression at 500 µm was identical for 300 and 1000 mW/mm^2, suggesting the presence of a ceiling effect for suppression at short distances. This may stem from the fact that in our CaMKII-Arch cross, only 64% of CaMKII+ cells express Arch, which could explain why suppression reaches a maximum of ~80% at short distances regardless of laser intensity.

Figure S4. Optogenetic suppression significantly changes gap termination response amplitude.

(Related to Figs. 1-3)

We suppressed multi-unit activity (300mW/mm^2) during the interval between presentations of a 10ms gap and the startle pulse. A) Suppressing SOM interneuron activity reliably increased GTR amplitudes, consistent with the increase in gap detection seen following post-gap suppression in awake behaving SOM mice. Significant increases in spiking activity were observed in 5 of 10 multi-unit sites exhibiting a GTR. B) Suppressing PV interneuron activity reliably increased GTR amplitudes, consistent with the increase in behavioral gap detection seen following post-gap suppression in awake SOM mice. Significant increases in spiking activity were observed in 5 of 8 sites exhibiting a GTR. C) As expected, suppressing CaMKII-expressing neurons decreased GTR amplitudes, consistent with the decrease in gap detection seen following suppression of excitatory activity during the post-gap interval. Significant decreases in spiking activity were observed in 5 of 10 sites at exhibiting a GTR.

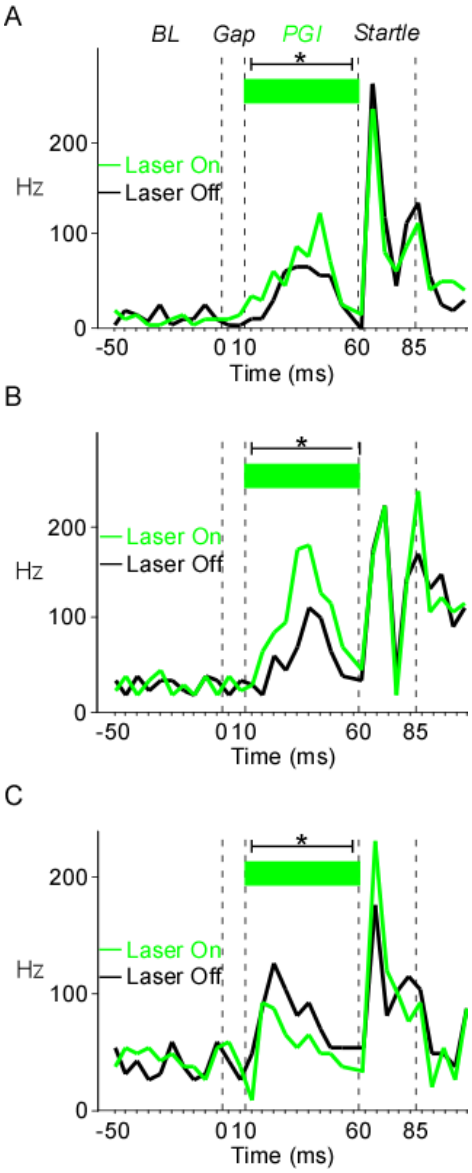

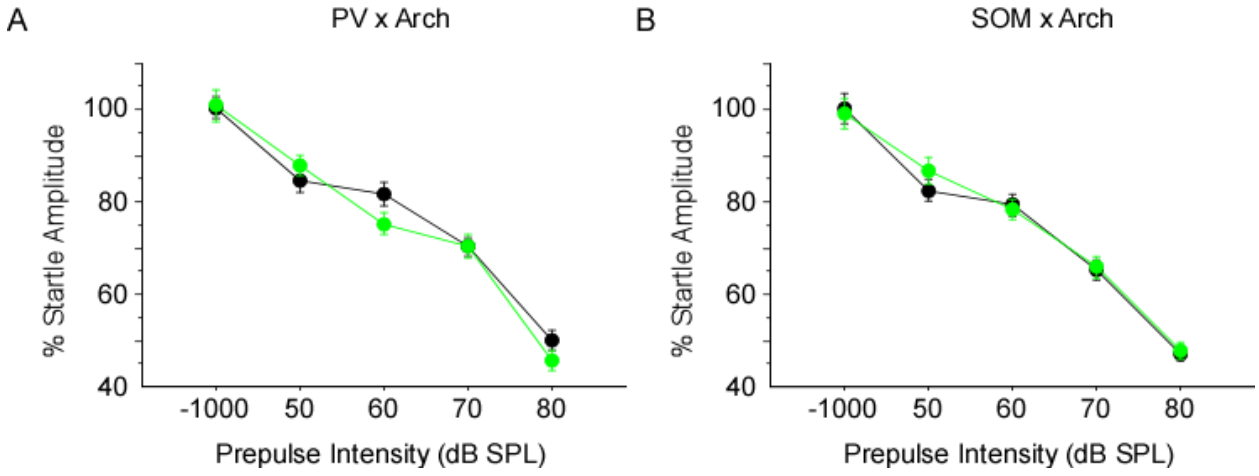

Figure S5. Optogenetic suppression of PV or SOM interneuron activity does not alter prepulse inhibition.

(Related to Figs. 1-2)

We measured prepulse inhibition in groups of PV (n=6 mice, 10 sessions) and SOM (n=4 mice, 7 sessions) mice. Prepulse intensities were 50-80 dB SPL, in 10dB steps. Startle responses were normalized to startle amplitudes associated with no prepulse ("none"). White noise prepulse (50ms) and startle stimuli (25ms, 100dB SPL) were separated by a 75ms silent interstimulus interval (ISI). Interleaved laser pulses suppressed interneuron activity during the prepulse and ISI. This manipulation had no impact on prepulse inhibition in PV (A) or SOM (B) mice. Note that even the quietest prepulse (50 dB) was well above the likely threshold for tone detection. It is possible that optogenetic manipulation could affect prepulse inhibition for prepulse intensities closer to threshold, just as optogenetic manipulation affects gap detection for brief but not long gaps.

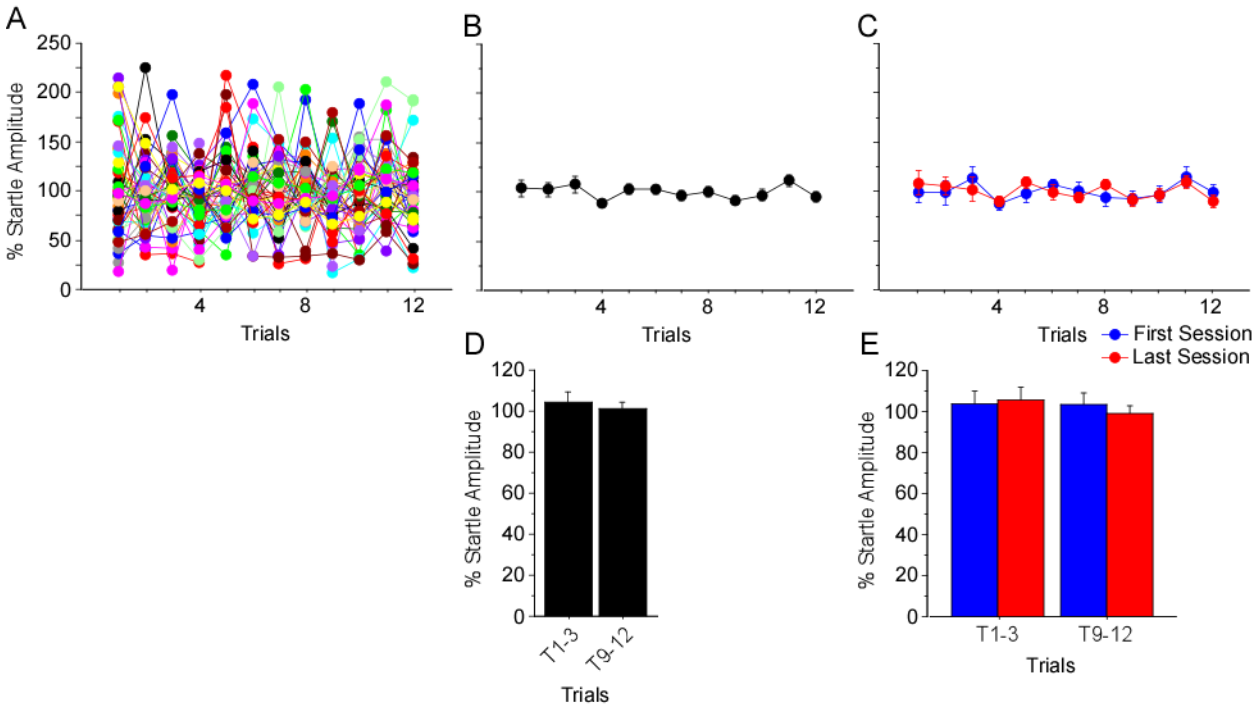

Figure S6. Mice do not show within-session habituation to the startle stimulus.

(Related to Experimental Procedures)

To test for habituation of startle responses, we examined startle amplitudes (for 0ms gaps, i.e. without a gap) over the course of the first and last session for each mouse. Startle amplitudes are normalized to the mean Gap 0ms startle amplitude, and include only data from laser "off" trials. Evidence of habituation would manifest as a change in Startle Amplitude across trials. A) Startle response amplitudes across trials for the first and last session for all mice. B-C) Startle amplitudes across 12 trials, averaged across animals, consistently fell within 20% of the mean, with no evidence of a decrease across trials, either for all sessions (B) or when plotting the first and last session means separately (C). Note that (B) is the mean of (A) across animals, and (C) is the data in (B) separated out into first and last sessions. D-E) A comparison (unpaired t-test) of the initial three (T1-3) versus the final three (T9-12) trials revealed no difference in startle amplitudes over the course of the session, both for all sessions combined (D; p = .53) or when sorting by first and last sessions (E; p = .99 and p = .35, respectively).

Table S1. Behavioral summary by silencing protocol and analysis.

Analysis of Variance	Post-gap silencing		Pre-gap silencing	Prolonged silencing
Intensity:	300mW/mm^2	1000mW/mm^2	300mW/mm^2	300mW/mm^2
SOM	M: p = .13 **I: p = .049**	**M: p = .0001** **I: p =.006**	**M: p = .031** **I: p = .005**	M: p = .35 I: p = .48
PV	**M: p = .046** I: p = .12	**M: p <.0001** I: p = .14	**M: p =.09** I: p = .53	M: p = .13 I: p = .27
CaMKII	M: p = .95 **I: p = .018**	**M: p = .002** I: p = .44	**M: p = .019** I: p = .35	M: p = .35 I: p = .42
Kolmogorov-Smirnoff				
SOM	**p = .047**	**p = .0002**	**p = .004**	p = .099
PV	**p = .025**	**p < .0001**	**p = .019**	p = .09
CaMKII	p = .36	**p = .008**	**p = .046**	p = .07
Mann-Whitney				
SOM	**p = .023**	**p < .0001**	**p = .0008**	p = .09
PV	**p = .019**	**p < .0001**	**p = .032**	**p = .023**
CaMKII	p = .59	**p = .002**	**p = .017**	p = .11

Table S1. Comparison of results using parametric and non-parametric tests.

(Related to Table 1)

A) Repeated-measures two-way ANOVA p-values, with significant values ($p<0.05$) shown in red. Note that startle response amplitudes did not have a normal distribution (based on the Lilliefors test for normality). The ANOVA test is very robust with respect to the assumption of normality [9-12], such that the validity of the analysis is only slightly affected by considerable deviations from normality [10]. To confirm this we ran two non-parametric tests that do not depend on the assumption of normality: B) the Kolmogorov-Smirnov (K-S) test, and C) the Mann-Whitney test. The pattern of results was largely similar but not identical across these three tests. The K-S results were the same as ANOVA with two exceptions: pre-gap PV suppression changed from nearly significant to significant, and post-gap CaMK2 became insignificant at 300mW/mm^2, but was still significant at 1000mW/mm^2. The Mann-Whitney results were the same as with the K-S test, with one exception: prolonged PV suppression became significant. We conclude that our results are largely, but not perfectly, robust to the choice of parametric or non-parametric statistical tests. M: ANOVA main effect; I: ANOVA interaction

Supplemental References

1. Guo, W., Chambers, A.R., Darrow, K.N., Hancock, K.E., Shinn-Cunningham, B.G., and Polley, D.B. (2012). Robustness of cortical topography across fields, laminae, anesthetic states, and neurophysiological signal types. J Neurosci *32*, 9159-9172.
2. Dean, I., Robinson, B.L., Harper, N.S., and McAlpine, D. (2008). Rapid neural adaptation to sound level statistics. J Neurosci *28*, 6430-6438.
3. Paxinos, G., and Franklin, K.B.J. (2001). The Mouse Brain in Stereotaxic Coordinates, 2nd Edition, (San Diego: Academic Press).
4. Chow, B.Y., Han, X., Dobry, A.S., Qian, X., Chuong, A.S., Li, M., Henninger, M.A., Belfort, G.M., Lin, Y., Monahan, P.E., et al. (2010). High-performance genetically targetable optical neural silencing by light-driven proton pumps. Nature *463*, 98-102.
5. Anikeeva, P., Andalman, A.S., Witten, I., Warden, M., Goshen, I., Grosenick, L., Gunaydin, L.A., Frank, L.M., and Deisseroth, K. (2012). Optetrode: a multichannel readout for optogenetic control in freely moving mice. Nat Neurosci *15*, 163-170.
6. Goshen, I., Brodsky, M., Prakash, R., Wallace, J., Gradinaru, V., Ramakrishnan, C., and Deisseroth, K. (2011). Dynamics of retrieval strategies for remote memories. Cell *147*, 678-689.
7. Madisen, L., Mao, T., Koch, H., Zhuo, J.M., Berenyi, A., Fujisawa, S., Hsu, Y.W., Garcia, A.J., 3rd, Gu, X., Zanella, S., et al. (2012). A toolbox of Cre-dependent optogenetic transgenic mice for light-induced activation and silencing. Nat Neurosci *15*, 793-802.
8. Swetter, B.J., Fitch, R.H., and Markus, E.J. (2010). Age-related decline in auditory plasticity: experience dependent changes in gap detection as measured by prepulse inhibition in young and aged rats. Behav Neurosci *124*, 370-380.
9. Tiku, M.L. (1971). Power function of F-test uncder non-normal situations. J Amer Statist Assoc, 913-916.
10. Zar, J.H. ed. (2010). Biostatistical analysis, 5 Edition (Upper Saddle River, N.J.: Prentice-Hall/Pearson).
11. Srivastava, A. (1959). Effects of non-normality on the power of the analysis of variance test. Biometrika, 114-122.
12. Box, G., and Anderson, S. (1955). Permutation theory in the derivation of robust criteria and the study of departures from assumption. J Royal Statist Soc, 1-34.